

Electromagnetically induced transparency and dark fluorescence in a cascade three-level Lithium molecule

Jianbing Qi¹ and A. Marjatta Lyyra²

¹*Department of Physics and Astronomy, Penn State University at Berks,
Tulpehocken Road, P.O. Box 7009, Reading, PA 19610 and*

²*Physics Department, Temple University, Philadelphia, PA 19112*

(Dated: July 18, 2018)

We observed electromagnetically induced transparency (EIT) and dark fluorescence in a cascade three-level diatomic Lithium system using Optical-Optical Double Resonance (OODR) spectroscopy. When a strong coupling laser couples the intermediate state $A^1\Sigma_u^+(v=13, J=14)$ to the upper state $G^1\Pi_g(v=11, J=14)$ of ${}^7\text{Li}_2$, the fluorescence from both $A^1\Sigma_u^+$ and $G^1\Pi_g$ states was drastically reduced as the weak probe laser was tuned through the resonance transition between the ground state $X^1\Sigma_g^+(v=4, J=15)$ and the excited state $A^1\Sigma_u^+(v=13, J=14)$. The strong coupling laser makes an optically thick medium transparent for the probe transition. In addition, The fact that fluorescence from the upper state $G^1\Pi_g(v=11, J=14)$ was also dark when both lasers were tuned at resonance implies that the molecules were trapped in the ground state. We used density matrix methods to simulate the response of an open molecular three-level system to the action of a strong coupling field and a weak probe field. The analytical solutions were obtained under the steady-state condition. We have incorporated the magnetic sublevel (M) degeneracy of the rotational levels in the lineshape analysis and report $|M|$ dependent lineshape splitting. The theoretical calculations are in excellent agreement with the observed fluorescence spectra. We show that the coherence is remarkably preserved even when the coupling field was detuned far from the resonance.

PACS numbers: 42.50.Gy, 42.50.Hz, 33.40.+f

I. INTRODUCTION

Multilevel atomic and molecular systems offer many possibilities for the investigation of coherence effects and quantum control of the interactions among the quantum participants. In recent years, substantial attention has been paid to the study of coherence effects in atomic and molecular systems [1, 2, 3, 4], such as coherent population trapping (CPT) [5, 6, 7], electromagnetic induced transparency (EIT) [8, 9, 10, 11], ultraslow propagation of light [12, 13], and Autler-Townes splitting [14, 15, 16, 17]. More and more experiments are shifted from atomic systems to molecular systems for more practical applications [18, 19]. The multitude of quantum levels of molecular systems provides rich coupling schemes and thus a test ground for the study of coherence effects in molecular systems. However, compared to atomic systems, molecules have small transition dipole moments. A general characteristic of molecular systems is that they have many relaxation pathways. This in turn makes these systems much more open compared to closed atomic systems where excited states decay channels are limited. Furthermore, the degeneracy of the energy levels and other complications make the observation of coherence effects considerably more challenging from an experimental point of view. The Rabi frequency, the key parameter, is proportional to the transition dipole moment matrix element and the coupling field amplitude. Thus cw laser experiments that involve small transition dipole moment matrix elements are therefore quite difficult. However, a judicious choice of laser wavelengths

and beam propagation geometry can help overcome the Doppler broadening [20]. The Autler-Townes splitting was observed in a high temperature diatomic Lithium gas using multiple resonance excitation to overcome the Doppler effect [16, 21]. Recently, EIT in ultracold atomic gases, and Autler-Townes splitting effect in ultra-cold molecule formation and detection have been reported [22, 23, 24]. The study of coherence effects in molecular systems is timely and important not only for fundamental understanding of these effects, but also for the practical applications. In this paper, we present the detailed experimental investigation and the corresponding theoretical analysis of electromagnetically induced transparency and dark fluorescence in a cascade three-level diatomic Lithium in an inhomogeneously broadened environment. We have incorporated the effect of the magnetic sublevel (M) degeneracy of the rotational levels in the lineshape analysis and report $|M|$ -dependent lineshape splitting. We show that the coherence is remarkably preserved even when the coupling field was detuned far from the resonance. The open property of molecular systems will be discussed in our theoretical calculation. We also demonstrate that the coupling laser field dependent splitting of the upper level can be used as a new method for measuring the molecular transition dipole moment matrix element [21].

The paper is organized as follows. In section II, we present the theoretical model and the derivation of the analytical expressions to account for the experiments. We describe the experimental observations in section III. The discussion of the theoretical calculations using the

experimental parameters is given in section IV. Finally, a summary is presented.

II. THEORETICAL FRAMEWORK

A. Density Matrix Equation of Motion.

The excitation scheme for a three-level molecular system interacting with two laser fields is indicated in Fig. 1(a). We consider a moving molecule situated in a travelling wave $\vec{E}_i(z, t) = \vec{e}_i E_i \cos(k_i z - \omega_i t)$. The Hamiltonian, H , is given by,

$$H = H_0 + H_{int}, \quad (1)$$

where

$$H_0 = \sum_{i=1}^3 \varepsilon_i |i\rangle\langle i| \quad (2)$$

is the molecular Hamiltonian, and ε_i is the energy eigenvalue of the isolated molecule in state $|i\rangle$. We assume $\varepsilon_1 = 0$ for simplicity and all other states are measured relative to state $|1\rangle$. The

$$H_{int} = \sum_{i \neq j} \langle i | (-\vec{\mu} \cdot \vec{E}) | j \rangle = - \sum_{i \neq j} \mu_{ij} E_i \quad (3)$$

is the dipole interaction Hamiltonian, and μ_{ij} is the transition dipole moment for a molecule undergoing $|i, v', J'\rangle \leftrightarrow |j, v, J\rangle$ transition. The evolution of the molecular density matrix for a molecule moving with velocity v is governed by the master equation [25],

$$\frac{\partial \rho}{\partial t} + \vec{v} \cdot \nabla \rho = -\frac{i}{\hbar} [H, \rho] + \left(\frac{\partial \rho}{\partial t} \right)_{inc}, \quad (4)$$

where the second term on the left hand-side represents the damping due to spontaneous emission and other irreversible processes.

Before we apply the density matrix formalism to interpret the experimental results, we have to consider the relaxation details of the level system in Fig. 1(a). The first laser L1 excites the 7Li_2 molecules from the ground state level $X^1\Sigma_g^+(v=4, J=15)$ (level $|1\rangle$) to the intermediate level $A^1\Sigma_u^+(v=13, J=14)$ (level $|2\rangle$), and the second laser L2 couples the $A^1\Sigma_u^+(v=13, J=14)$ to the upper excited state $G^1\Pi_g(v=11, J=14)$ (level $|3\rangle$). Molecules in any specific rovibrational level of an excited electronic state can decay to many other rovibrational levels of lower electronic states, and only part of them decay back to their initial state. The upper excited electronic state $G^1\Pi_g$ can decay to two lower electronic states of $B^1\Pi_u$ and $A^1\Sigma_u^+$. The $A^1\Sigma_u^+$ state is the first singlet excited electronic state of the Lithium molecule. Molecules in a rovibrational level of the $A^1\Sigma_u^+$ state can decay to vibrational levels of the ground electronic state

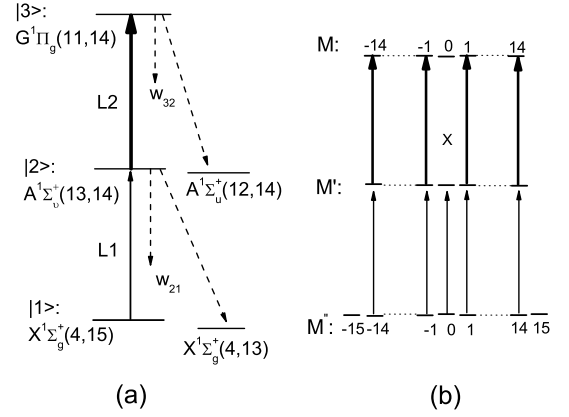


FIG. 1: 7Li_2 three-level cascade scheme: (a) The weak probe laser, L1 ($15642.636 \text{ cm}^{-1}$), was used to excite molecules from the ground state level $X^1\Sigma_g^+(v=4, J=15)$ to an excited intermediate level $A^1\Sigma_u^+(v=13, J=14)$. The laser, L2 ($17053.954 \text{ cm}^{-1}$), coupled the intermediate level to a higher electronic state level $G^1\Pi_g(v=11, J=14)$. The fluorescence from $A^1\Sigma_u^+(v=13, J=14)$ to $X^1\Sigma_g^+(v=4, J=13)$ and $G^1\Pi_g$ to $A^1\Sigma_u^+(v=12, J=14)$ were monitored. (b) The coupling details of the magnetic sublevels ($M=-J, -J-1, \dots, J-1, J$) of (a): For linearly polarized light, the selection rules require $\Delta M = 0$, thus The $M'' = \pm 15$ of the ground state levels are decoupled from the first transition (P transition: $\Delta J = -1$), while there is no $M = 0 \rightarrow M' = 0$ coupling for the upper transition (Q transition: $\Delta J = 0$).

$X^1\Sigma_g^+$. In the sense of the description of the total decay rate of level $|3\rangle$ to other energy levels, there is no difference between $B^1\Pi_u$ and $A^1\Sigma_u^+$ state.

We assume that the total radiative decay rate of the excited states $|2\rangle$ and $|3\rangle$ are γ_2 and γ_3 , respectively. The branching ratios b_2 and b_3 stand for the percentage of molecules in the level $|2\rangle$ and the level $|3\rangle$ that decay back to the ground-state $|1\rangle$ and level $|2\rangle$, respectively. When the branching ratios are equal to unity the three-level system is closed. The laser frequency detunings for a stationary molecule are defined as

$$\delta_1 = \omega_1 - \omega_{21}, \quad (5)$$

and

$$\delta_2 = \omega_2 - \omega_{32}, \quad (6)$$

where $\omega_{ij} = \frac{\varepsilon_i - \varepsilon_j}{\hbar}$ is the resonance transition frequency between $|i\rangle$ and $|j\rangle$. The Rabi frequency of the corresponding laser field is defined as:

$$g_i = \mu_{ij} E_i / \hbar. \quad (7)$$

We assume that the population of the ground state $|1\rangle$ has been replenished at the rate Λ , and only the ground-state is replenished. The laser beam has a finite beam size and therefore the transverse motion of molecules can

remove molecules from the interaction region before decay. This will introduce an effective additional relaxation of the excited states and the ground state. In order to account for this transit time, we simulate it with an effective decay rate w ($w \ll \gamma_i$) for all populations and polarizations. Then, the explicit form of equation (4) is

$$\left(\frac{\partial}{\partial t} + v_z \frac{\partial}{\partial z}\right) \varrho_{33} = ig_2 \cos(k_2 z - \omega_2 t) (\varrho_{32} - \varrho_{23}) - (\gamma_3 + w) \varrho_{33}, \quad (8)$$

$$\begin{aligned} \left(\frac{\partial}{\partial t} + v_z \frac{\partial}{\partial z}\right) \varrho_{22} = & -ig_2 \cos(k_2 z - \omega_2 t) (\varrho_{32} - \varrho_{23}) \\ & -ig_1 \cos(k_1 z - \omega_1 t) (\varrho_{12} - \varrho_{21}) \\ & + W_{32} \varrho_{33} - (\gamma_2 + w) \varrho_{22}, \end{aligned} \quad (9)$$

$$\left(\frac{\partial}{\partial t} + v_z \frac{\partial}{\partial z}\right) \varrho_{11} = ig_1 \cos(k_1 z - \omega_1 t) (\varrho_{12} - \varrho_{21}) - \Lambda + W_{21} \varrho_{22} - w \varrho_{11}, \quad (10)$$

$$\begin{aligned} \left(\frac{\partial}{\partial t} + v_z \frac{\partial}{\partial z}\right) \varrho_{32} = & ig_2 \cos(k_2 z - \omega_2 t) (\varrho_{33} - \varrho_{22}) \\ & + (-i\omega_{32} - \gamma_{32} - w) \varrho_{32} \\ & + ig_1 \cos(k_1 z - \omega_1 t) \varrho_{31}, \end{aligned} \quad (11)$$

$$\begin{aligned} \left(\frac{\partial}{\partial t} + v_z \frac{\partial}{\partial z}\right) \varrho_{31} = & [-i\omega_{31} - (\gamma_{31} + w)] \varrho_{31} \\ & - ig_2 \cos(k_2 z - \omega_2 t) \varrho_{21} \\ & + ig_1 \cos(k_1 z - \omega_1 t) \varrho_{32}, \end{aligned} \quad (12)$$

$$\begin{aligned} \left(\frac{\partial}{\partial t} + v_z \frac{\partial}{\partial z}\right) \varrho_{21} = & [-i\omega_{21} - (\gamma_{21} + w)] \varrho_{21} \\ & + ig_1 \cos(k_1 z - \omega_1 t) (\varrho_{22} - \varrho_{11}) \\ & - ig_2 \cos(k_2 z - \omega_2 t) \varrho_{31}, \end{aligned} \quad (13)$$

where the W_{ij} is the population decay rate from level $|i\rangle$ to $|j\rangle$, $W_{32} = b_3 \gamma_3$, and $W_{21} = b_2 \gamma_2$, and γ_{ij}^c represents the collisional dephasing rate. The polarization decay rate γ_{ij} is given by

$$\gamma_{ij} = \gamma_{ji} = \frac{1}{2} \sum_k (W_{ik} + W_{ki}).$$

Let

$$\Delta_1 = \omega_1 - \omega_{12} - k_1 v_z = \delta_1 - k_1 v_z, \quad (14)$$

and

$$\Delta_2 = \omega_2 - \omega_{23} - k_2 v_z = \delta_2 - k_2 v_z, \quad (15)$$

where v_z is the velocity component of the molecule in the laser propagation direction. Equations (8)-(13) can be changed into ones for the density-matrix elements of the slowly varying function of time and space by setting

$$\varrho_{21} = \rho_{21} e^{i(k_1 z - \omega_1 t)}, \quad (16)$$

$$\varrho_{32} = \rho_{32} e^{i(k_2 z - \omega_2 t)}, \quad (17)$$

$$\varrho_{31} = \rho_{31} e^{i[(k_1 + k_2)z - (\omega_1 + \omega_2)t]}. \quad (18)$$

After applying the rotating wave approximation, the above equations (8)-(13) can be written as:

$$\frac{d\rho_{33}}{dt} = i\frac{g_2}{2}(\rho_{32} - \rho_{23}) - (\gamma_3 + w)\rho_{33}, \quad (19)$$

$$\begin{aligned} \frac{d\rho_{22}}{dt} = & i\frac{g_1}{2}(\rho_{21} - \rho_{12}) - i\frac{g_2}{2}(\rho_{32} - \rho_{23}) \\ & - (\gamma_2 + w)\rho_{22} + W_{32}\rho_{33}, \end{aligned} \quad (20)$$

$$\frac{d\rho_{11}}{dt} = i\frac{g_1}{2}(\rho_{12} - \rho_{21}) + W_{21}\rho_{22} - w\rho_{11} + \Lambda, \quad (21)$$

$$\begin{aligned} \frac{d\rho_{32}}{dt} = & i\frac{g_2}{2}(\rho_{33} - \rho_{22}) + i\frac{g_1}{2}\rho_{31} + i\Delta_2\rho_{32} \\ & - (\gamma_{23} + w)\rho_{32}, \end{aligned} \quad (22)$$

$$\begin{aligned} \frac{d\rho_{31}}{dt} = & i\frac{g_1}{2}\rho_{32} - i\frac{g_2}{2}\rho_{21} - (\gamma_{13} + w)\rho_{31} \\ & + i(\Delta_1 + \Delta_2)\rho_{31}, \end{aligned} \quad (23)$$

$$\begin{aligned} \frac{d\rho_{21}}{dt} = & i\frac{g_1}{2}(\rho_{22} - \rho_{11}) - i\frac{g_2}{2}\rho_{31} + i\Delta_1\rho_{21} \\ & - (\gamma_{12} + w)\rho_{21}, \end{aligned} \quad (24)$$

In the steady-state limit, we can solve the above equations iteratively for the population (ρ_{ii}) of each level to the lowest order of the weak probe laser Rabi frequency g_1 , but to all orders in g_2 . After some lengthy algebra, we obtain the non-normalized analytical solutions for the populations of the two excited states:

$$\rho_{22} = -\frac{g_1^2 \rho_{11}^{(0)}}{2D(\Delta_2)} \text{Im} \left\{ \frac{\frac{g_2^2}{4} \left(1 - \frac{W_{32}}{\gamma_3 + w}\right) [\Delta_2 - i(\gamma_{32} + w)] + A[\Delta_1 + \Delta_2 + i(\gamma_{31} + w)]}{[\Delta_1 + i(\gamma_{21} + w)][\Delta_1 + \Delta_2 + i(\gamma_{31} + w)] - \frac{g_2^2}{4}} \right\}, \quad (25)$$

and

$$\rho_{33} = \frac{g_1^2 g_2^2 \rho_{11}^{(0)}}{8D(\Delta_2)(\gamma_3 + w)} \text{Im} \left\{ \frac{-2(\gamma_{32} + w)[\Delta_1 + \Delta_2 + i(\gamma_{31} + w)] + (\gamma_2 + w)[\Delta_2 - i(\gamma_{32} + w)]}{[\Delta_1 + i(\gamma_{21} + w)][\Delta_1 + \Delta_2 + i(\gamma_{31} + w)] - \frac{g_2^2}{4}} \right\}, \quad (26)$$

where

$$A = \Delta_2^2 + (\gamma_{32} + w)^2 + \frac{g_2^2(\gamma_{32} + w)}{2(\gamma_3 + w)},$$

$$D(\Delta_2) = A(\gamma_2 + w) + \frac{g_2^2(\gamma_{23} + w)}{2} \left(1 - \frac{W_{32}}{\gamma_3 + w}\right),$$

and $\rho_{11}^{(0)} = \frac{\Lambda}{w}$ is the initial population without the probe laser field. We can see that the system will be ideally closed if $W_{32} = \gamma_3 + w$, and the expressions will be greatly simplified.

B. Doppler Effect

Let us assume that two laser beams counter propagate along the z axis, the probe laser travels to the right (positive), and the coupling laser to the left (negative). Due to the Doppler effect, a molecule moving with a positive velocity v_z with respect to the rest frame will see the probe laser and coupling laser frequencies ω_1 , and ω_2 , respectively, as:

$$\omega_1(v_z) = \omega_1 - \frac{v_z}{c}\omega_1, \quad (27)$$

and

$$\omega_2(v_z) = \omega_2 + \frac{v_z}{c}\omega_2. \quad (28)$$

We define the velocity dependent detunings as

$$\Delta_1(v_z) = \delta_1 - \frac{v_z}{c}\omega_1, \quad (29)$$

and

$$\Delta_2(v_z) = \delta_2 + \frac{v_z}{c}\omega_2. \quad (30)$$

The velocity dependent laser detunings can be expressed in laser frequency detuning and the transition frequency as follow:

$$\Delta_1(v_z) = \left(1 - \frac{v_z}{c}\right)\delta_1 - \frac{v_z}{c}\omega_{12}, \quad (31)$$

and

$$\Delta_2(v_z) = \left(1 + \frac{v_z}{c}\right)\delta_2 + \frac{v_z}{c}\omega_{23}. \quad (32)$$

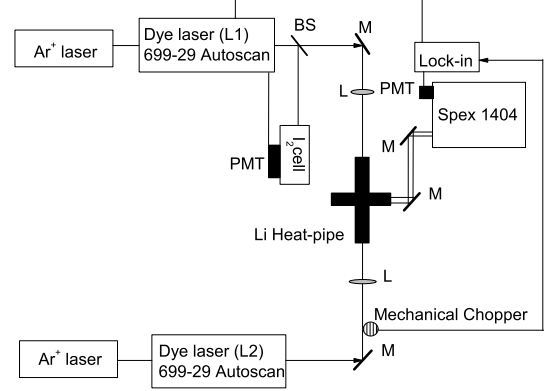


FIG. 2: Experimental set-up: Two linearly polarized counter propagating laser beams were aligned coaxially, and were focused at the center of the Lithium heat-pipe. The fluorescence was collected and focused to the monochromator (SPEX 1404) from the side window. The signal was amplified by the lock-in amplifier and the output was recorded on the Coherent 699-29 Autoscan computer. (M: Mirror, BS: Beam splitter, L: Lens, PMT: Photo-multiplier)

At thermal equilibrium, the molecules in a gas phase follow the Maxwellian velocity distribution, in one dimension, which is given as [26]:

$$N(v_z) = \frac{1}{\sqrt{\pi}u_p} \exp\left(-\frac{v_z^2}{u_p^2}\right), \quad (33)$$

where $u_p = \left(\frac{2kT}{m}\right)^{1/2}$ is the most probable velocity of the molecules, k is the Boltzmann's constant, m is the mass of a molecule, and T is the temperature. The experimental observations should be the sum ρ_{ii} for all velocity groups.

$$\langle \rho_{ii} \rangle_{Doppler} = \int_{-\infty}^{+\infty} \rho_{ii} N(v_z) dv_z. \quad (34)$$

C. $|M|$ -Dependent Rabi Frequency

For each rotational angular momentum J , there are $2J+1$ magnetic sublevels, $M=-J, -(J-1), \dots, J-1, J$, which specify the projection of the total angular momentum J along a laboratory fixed Y-axis. The interaction of each magnetic sublevel with the laser field depends not only

on the transition (P, Q, or R) but also on the polarization of the laser field [27, 28]. The Rabi frequency g_i for each laser field and for a given molecular transition of $(v', J') \leftarrow (v, J)$ can be written in the form:

$$g_i = \mu_{ij} E_i / \hbar = \langle v' | \mu_e | v \rangle f(J' J M' M; \Lambda' \Lambda) E_i / \hbar, \quad (35)$$

where μ_e is the electronic transition dipole moment, $\mu_e = \langle \Lambda' | \mu | \Lambda \rangle$, $f(J' J M' M; \Lambda' \Lambda)$ is the rotational line strength factor for transition $|J' M' \Lambda' \rangle \leftrightarrow |J M \Lambda \rangle$, and E_i is the laser field strength. For a linearly polarized laser field, the rotational line strength factor for the $Q(\Delta J = J - J' = 0)$ transition is

$$f_Q = \frac{|M|}{\sqrt{J(J+1)}}, \quad (36)$$

and for the $P(\Delta J = J - J' = -1)$ transition,

$$f_P = \sqrt{\frac{(J^2 - M^2)}{(2J+1)(2J-1)}}. \quad (37)$$

For linearly polarized light, the transition selection rules require $\Delta M = M' - M = 0$, thus there is no $M = 0 \rightarrow M' = 0$ coupling for upper transition. The $M'' = \pm 15$ of the ground state are decoupled from the first transition also. The coupling of the three-level configuration of the Fig. 1(a) can be viewed as 28 M -dependent couplings for L2 and 29 couplings for L1, as shown in Fig. 1(b). The Rabi frequency depends on the absolute value of the magnetic sublevel $|M|$. This results in $|M|$ -dependent population expressions of equation (25) and (26) also. The observed fluorescence signal, apart from a proportionality factor, can be calculated by integrating the ρ_{ii} over the velocity distribution and summing over all $|M|$, i.e.

$$\rho_{ii}(\delta_1, \delta_2) \propto \sum_{|M|} \int_{-\infty}^{+\infty} \rho_{ii} N(v_z) dv_z. \quad (38)$$

III. EXPERIMENTAL RESULTS

The experimental set-up is shown in Fig. 2. This is a typical Optical-Optical Double Resonance (OODR) scheme. Lithium molecules are generated in a five-arm stainless steel oven with the temperature around 1000 Kelvin, and with Argon buffer gas pressure around 100-300 mTorr. Two Coherent 699-29 Autoscan dye lasers were used to produce the required laser wavelengths. Two linearly polarized laser beams were arranged in counter-propagating configuration and aligned coaxially.

We monitored the population of the intermediate state $A^1\Sigma_u^+(v = 13, J = 14)$ (level $|2 \rangle$) by detecting its fluorescence to the ground-state rovibrational level

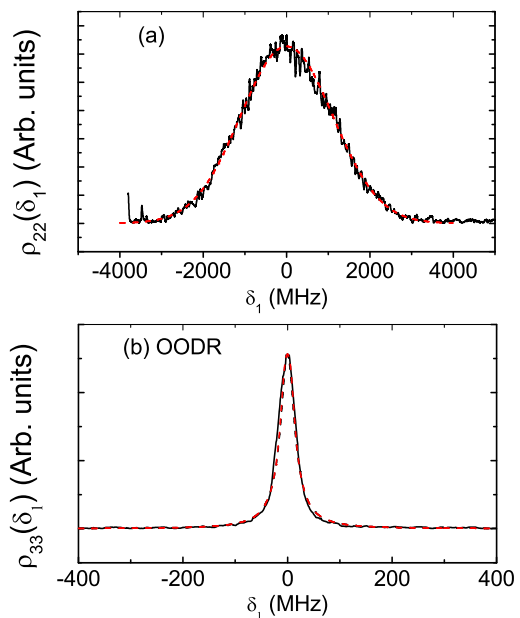


FIG. 3: (color online) (a) The Doppler broadened fluorescence spectrum of $A^1\Sigma_u^+(13, 14)$ to $X^1\Sigma_g^+(4, 13)$ is plotted as a function of the detuning of the probe laser without the coupling laser. (b) Measured OODR signal of $G^1\Pi_g(11, 14)$ along with the calculation with 1 mW coupling laser power. (Solid lines: experiment, dashed lines: calculation.)

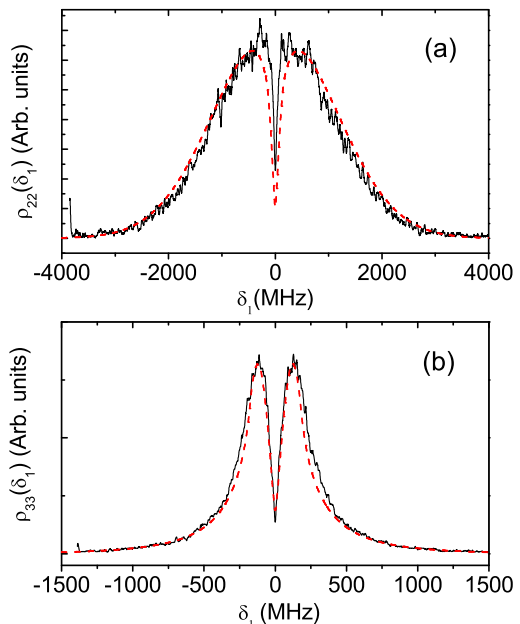


FIG. 4: (color online) Measured experimental spectra along with the calculations. (a) Fluorescence from level $|2 \rangle$. (b) Fluorescence from level $|3 \rangle$. The fitting parameters are: $\langle v' | \mu_e | v \rangle = 1.45(\pm 0.1) a.u.$, $\gamma_{i3}^1 = \gamma_{23}^2 = 1 MHz$, $\gamma_{i2}^5 = 5 MHz$. The coupling laser power is 480 mW. (Solid lines: experimental, dashed lines: calculation.)

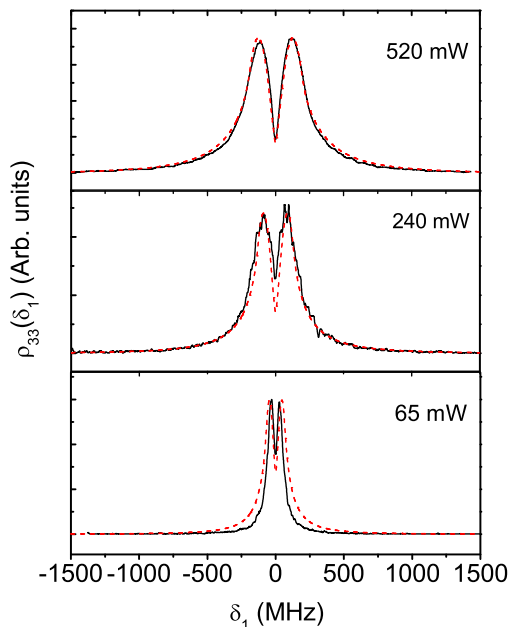


FIG. 5: (color online) Measured fluorescence spectra of the upper level as a function of the probe laser detuning (δ_1) for different coupling laser power with the coupling laser frequency tuned at resonance ($\delta_2 = 0$). The fitting parameters are the same as in Fig. 4: $\langle v' | \mu_e | v \rangle = 1.45(\pm 0.1) a.u.$, $\gamma_{13}^c = \gamma_{23}^c = 1 MHz$, $\gamma_{12}^c = 5 MHz$. (solid lines: experimental, dashed lines: calculation)

$X^1\Sigma_g^+(v = 4, J = 13)$. The corresponding wavelength is 6377.83 \AA in air. The population of the upper state $G^1\Pi_g(v = 11, J = 14)$ (level $|3\rangle$) was monitored by detecting its fluorescence to the $A^1\Sigma_u^+(v = 12, J = 14)$ state with the wavelength of 5791.30 \AA in air. The fluorescence was collected and focused to the monochromator (SPEX 1404) through a set of mirrors from the side window of the heat-pipe oven. The selected fluorescence was detected by a cooled photomultiplier (PMT) at the exit slit of the SPEX when the monochromator was set to the corresponding spontaneous emission wavelength. The PMT signal was amplified by a lock-in amplifier (SR 850), and the output was recorded on the 699-29 Autoscan computer while the probe laser (L1) frequency was scanned. All laser frequencies were calibrated to $\pm 0.002 cm^{-1}$ with the standard Iodine spectra [29]. The first transition from the ground state level of ${}^7Li_2 X^1\Sigma_g^+(v = 4, J = 15)$ to the excited state $A^1\Sigma_u^+(v = 13, J = 14)$ is driven by the probe laser L1, while the transition from $A^1\Sigma_u^+(v = 13, J = 14)$ to the upper state level $G^1\Pi_g(v = 11, J = 14)$ is driven by laser L2. In the absence of laser L2, a frequency scan of the probe laser L1 yields the usual Doppler broadened fluorescence spectrum of the $A^1\Sigma_u^+(v = 13, J = 14)$ as shown in the Fig. 3(a). If the coupling laser

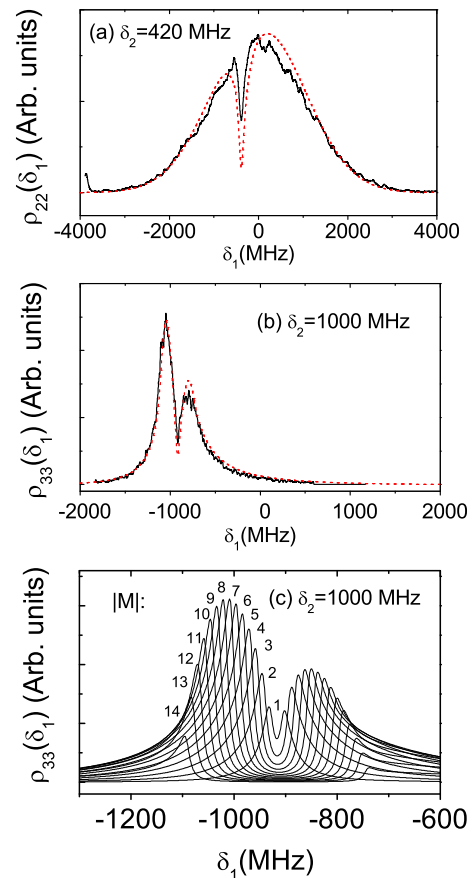


FIG. 6: (color online) Fluorescence spectra for the coupling laser detuned from the resonance frequency: The coupling laser power is same as that in Fig. 4. (a) The coupling laser is detuned at $\delta_2 = 420 MHz$ above the resonance frequency. The EIT dip of level $|2\rangle$ shifted by $385 MHz$ below the resonance frequency. (b) The coupling laser is detuned $1.0 GHz$ above the resonance frequency. The splitting of the upper state $|3\rangle$ is still preserved, but shifted $917 MHz$ below the resonance frequency. (Solid lines: experiment, dashed lines: calculation) (c) Calculated 14 $|M|$ -components of (b) before summation using Eq. (38).

L2 is weak and set at the resonance transition of the $A^1\Sigma_u^+(v = 13, J = 14)$ to $G^1\Pi_g(v = 11, J = 14)$, by monitoring the fluorescence of $G^1\Pi_g(v = 11, J = 14)$ to $A^1\Sigma_u^+(v = 12, J = 14)$, a scan of the probe laser from $X^1\Sigma_g^+(v = 4, J = 15)$ to $A^1\Sigma_u^+(v = 13, J = 14)$ leads to the usual OODR spectrum for the upper state, $G^1\Pi_g(v = 11, J = 14)$, as shown in Fig. 3(b). Upon increasing the coupling laser power, a sharp dip emerges at the center of the Doppler broadened fluorescence spectrum of the $A^1\Sigma_u^+(v = 13, J = 14)$, as shown in Fig. 4(a). One may naively interpret the emergence of that dip as the consequence of the additional transfer of population to the upper level $G^1\Pi_g(v = 11, J = 14)$ by the

strong coupling laser. However, a sharp dip also appears in the middle of the OODR fluorescence signal of the upper $G^1\Pi_g(v = 11, J = 14)$ level. The OODR fluorescence peak, splits into two components as shown in Fig. 4(b). The fluorescence of both excited states is drastically reduced under the action of the strong coupling laser (L2). Because the intensity of the fluorescence is proportional to the population of the corresponding excited state, the origin of the fluorescence dips is based on the fact that the molecules can not be excited by the probe laser and the coupling laser to either the intermediate level $A^1\Sigma_u^+(v = 13, J = 14)$ or the upper level $G^1\Pi_g(v = 11, J = 14)$ from the ground-state under a strong coupling laser. Since the strong coupling laser L2 modified the transition from $X^1\Sigma_g^+(v = 4, J = 15)$ to $A^1\Sigma_u^+(v = 13, J = 14)$, the ground state molecules can not absorb the probe laser photons and be excited to the excited state $A^1\Sigma_u^+(v = 13, J = 14)$ at the resonance frequency. The remarkable result is that the second transition does not transfer the molecules to the higher excited $G^1\Pi_g$ state either. The experimental results also show that the stronger the coupling laser is, the deeper and wider are the dips as shown in Fig. 5. In a sense of the first transition, the molecule becomes transparent under the action of the strong coupling laser (electromagnetically induced transparency) and thus the molecules must stay in the ground state.

IV. DISCUSSION

In order to carry out a comparison between the experimental spectra and the theory, we calculate Eq. (38) based on Eq. (25) and Eq. (26) using the experimental data for the transition frequencies ω_{21} and ω_{32} . The lifetimes of level $|2\rangle$ ($\tau_2 = 1/\gamma_2$) and $|3\rangle$ ($\tau_3 = 1/\gamma_3$) were based on the references [30, 31]. These values are 18 ns, and 16.15 ns, respectively. From Fig. 3(a) (the probe laser scan) we obtained the most probable molecular velocity by measuring the Doppler line-width, which is 2.6 GHz. The coupling beam waist ($1/e^2$) is $360\ \mu\text{m}$. The weak probe laser beam is $222\ \mu\text{m}$ ($\sim 1\ \text{mW}$). The transit rate (w) of the molecules entering and leaving the interaction region can be estimated according to reference [32] and is $\sim 2\ \text{MHz}$. The branching ratios b_2 and b_3 can be estimated from the Franck Condon factor calculation to be 0.1 and 0.2, respectively. We perform the calculations based on the analytical solution of Eq. (26) by searching the value of the transition dipole moment matrix element and the γ_{ij}^c to best match the experimental spectrum of ρ_{33} in Fig. 4(b). The resulting value of the transition dipole moment matrix element $\langle v'|\mu_e|v\rangle$ for $G^1\Pi_g - A^1\Sigma_u^+$ is $1.45 (\pm 0.1)$ a.u.. After the completion of this step, we calculate the corresponding spectrum of ρ_{22} , which is again in good agreement with the experimental spectrum shown in Fig. 4(a) as dashed lines. However,

the experimental dip is much narrower than the theoretical calculation. Both the theory and the experimental spectra clearly show that a strong coupling laser modified the transitions. The molecules stay in the ground state even though the laser (L1) was tuned to the resonance of the first transition as long as the coupling laser (L2) couples the upper transition with adequate coupling strength (g_2). The optically opaque molecular gas now becomes transparent for laser L1 (EIT). Again, the dip is not due to the population transfer to the upper state $|3\rangle$ by the coupling laser L2, because the upper state has no population either. The fluorescence of both excited states becomes dark in the presence of the strong coupling laser. Keeping all parameters fixed, decreasing the strength of the coupling laser, we obtain the single peak OODR for ρ_{33} as shown by the dashed lines in Fig. 3(b). The calculated ρ_{22} without the coupling laser is identical to the Doppler broadened profile as shown in Fig. 3(a).

As indicated in the equation (25) and (26) that the Rabi frequency of the coupling field g_2 , has a dominant influence on the depth and width of the dips of ρ_{33} once $g_2^2 \gg 4(\gamma_{21} + w)(\gamma_{31} + w)$. The decay rate of the upper level $|3\rangle$ and the branching ratios b_i , have a contribution to the depth of the dip of the spectra as well. The branching ratio b_i , the collision rate γ_{ij}^c and the transit rate w have a dominant contribution to the linewidth and the wings of the upper state spectra. This is understandable and expected compared to a closed system. A large γ_{ij}^c means that the coherence will be destroyed quickly, and a large transit rate w implies an effective shorter lifetime of the excited levels, while small values of w and large branching ratios imply that the system is better described by a closed system. The dip of ρ_{22} is none zero since the P transition of the probe laser can populate the M=0 sublevel of $A^1\Sigma_u^+$ state, while the coupling field transition is a Q transition, the M=0 level is decoupled from the coupling field transition (see Fig. 1(b)). Also, the Doppler broadening greatly reduces the width of the transparency window.

When the coupling laser is off resonance, the dips are still preserved as long as the coupling field is strong enough. However, the position of the dips will change to the opposite side of the detuning of the coupling field (δ_2). We can easily find, by checking the integral equation (34), that the position of the dip is at the modified two-photon transition: $\delta_1 = -|\frac{k_1}{k_2}|\delta_2$ due to the Doppler effect, and at $\delta_1 = -\delta_2$ for Doppler free case. This is a completely coherent process, since the detuning of L2 prevents the population buildup on level $|3\rangle$. The splitting of this component depends on the coupling field strength and the detuning of δ_2 as well as the linewidths of the two excited states. Two experimental spectra with coupling laser detuned from the resonance by 420 MHz, and 1.0 GHz, respectively, but with the same laser intensity as in the Fig. 4 are shown in Fig. 6(a)-(b), which show

that the coherence is robustly preserved. We plot 14 $|M|$ sublevel components of Fig. 6(b) in an expanded scale to show the $|M|$ -dependent splitting by using equations (26), and (34) in Fig. 6(c). For a Q transition the splitting of each $|M|$ component is proportional to the value of $|M|$.

V. SUMMARY

In summary, we have observed the electromagnetically induced transparency (EIT) and dark fluorescence in an inhomogeneous broadened Lithium molecular system. The power dependent upper state splitting spectrum provides a useful method to experimentally measure the transition dipole moment matrix element. The value of this parameter from fits of the experimental spectra agrees very well with the theoretical calculation. It could provide new insights into the electronic structures and dynamics of Rydberg states [21]. In the fitting of the experimental spectra we find that the branching ratio value can be varied over a large range and still give a reasonable fit. It implies that it is possible to observe EIT in a very open system, such as pre-dissociated molecular states. We demonstrated that the coherence was remarkably preserved even when the coupling field was detuned far from the resonance. We have discussed a systematic approach to the treatment of the response of a three-level open molecular system to the presence of two laser fields. The theoretical model and the treatment of the degeneracy of the rotational levels agree very well with the experimental spectra.

ACKNOWLEDGEMENTS

We thank Profs. L. M. Narducci and F. C. Spano for their valuable discussions, as well as A. Lazoudis, T. Kirova and J. Magnes for their technical help in the lab. J. Qi is grateful for the summer research support from Penn State University at Berks. We acknowledge support from NSF grants PHY0245311 and PHY9983533 to Temple University .

-
- [1] M. O. Scully, and M. Fleischhauer, *Science* 263, 337(1994).
 - [2] G. Vemuri, G. S. Agarwal, and B. D. Nageswara Rao, *Phys. Rev. A* 53, 2842(1996).
 - [3] R. Sussmann et al., *J. Chem. Phys.* 103, 3315(1995); T. Halgmann et al., *J. chem. Phys.* 104, 7068(1996).
 - [4] K. Ichimura, K. Yamamoto, N. Gemma, *Phys. Rev. A* 58, 4116(1998).

- [5] For a review of this subject, see E. Arimondo, in *Progress in Optics XXXV*, edited by E. Wolf (North-Holland, Amsterdam, 1996).
- [6] H. Y. Ling, Y. Q. Li, M. Xiao, *Phys. Rev. A* 53, 1014(1995).
- [7] O. Schmidt, R. Wynands, Z. Hussein, and D. Meschede, *Phys. Rev. A* 53, R27(1996).
- [8] S. E. Harris, *Phys. Today* 50, 736(1997).
- [9] M. Fleischhauer, and M. D. Lukin, *Phys. Rev. Lett.* 84, 5094(2000).
- [10] S. A. Hopkins, E. Usadi, H. X. Chen, A. V. Durrant, *Opt. Comm.* 138, 185-192(1997).
- [11] N. E. Karapanagioti, O. Faucher, Y.L. Shao, D. Charalambidis, H. Bachau, E. Cormier, *Phys. Rev. Lett.* 74, 2431(1995).
- [12] L. V. Hau et al., *Nature (London)* 397, 594(1999).
- [13] M. M. Kash et al., *Phys. Rev. Lett.* 82, 5229(1999); D. Budker, D. F. Kimball, S. M. Rochester, and V. V. Yashchuk, *Phys. Rev. Lett.* 83, 1767(1999); M. D. Lukin, A. B. Matsko, M. Fleischhauer, and M.O Scully, *Phys. Rev. Lett.* 82, 1847(1999).
- [14] F. C. Spano, *J. Chem. Phys.* 114, 276(2001).
- [15] F. Renzoni, A. Lindner, and E. Arimondo, *Phys. Rev. A* 60, 450(1999).
- [16] J. Qi, G. Lazarov, X. Wang, L. Li, L. M. Narducci, A. M. Lyyra, and F. C. Spano, *Phys. Rev. Lett.* 83, 288(1999).
- [17] R. Garcia-Fernandez, A. Ekers, J. Klavins, L. P. Yatsenko, N. B. Nikolai, B. W. Shore, and K. Bergmann, *Phys. Rev. A* 71, 023401 (2005).
- [18] F. Benabid, P. S. Light, F. Couny, and P. S. Russell, *Optics Express* 13 (15): 5694-5703(2005).
- [19] S. Ghosh, J. E. Sharping, D. G. Ouzounov, and A. L. Gaeta, *Phys. Rev. Lett.* 94, 093902(2005).
- [20] A. Lazoudis et al., submitted to *Phys. Rev. Lett.*; also arXiv:quant-ph/0508110v1 15 August 2005.
- [21] J. Qi, F. C. Spano, T. Kirova, A. Lazoudis, J. Magnes, L. Li, L. M. Narducci, R. W. Field, and A. M. Lyyra, *Phys. Rev. Lett.* 88, 173003(2002).
- [22] F. S. Cataliotti, C. Fort, T. W. Hansch, M. Inguscio, and M. Prevedelli, *Phys. Rev. A* 56, 2221(1997).
- [23] B. Laburthe Tolra, C. Drag, and P. Pillet, *Phys. Rev. A* 64, 061401(R)(2001).
- [24] U. Schloder, T. Deuschle, C. Silber, and C. Zimmermann, *Phys. Rev. A* 68, 051403(R)(2003).
- [25] S. Stenholm, *Foundations of Laser Spectroscopy* (Wiley Interscience, New York, 1984).
- [26] W. Demtroder, *Laser Spectroscopy* (Springer-Verlag, Berlin, 1982).
- [27] Y. B. Band, and P. S. Julienne, *J. Chem. Phys.* 94, 5291(1991).
- [28] Y. B. Band, and P. S. Julienne, *J. Chem. Phys.* 97, 9107(1992).
- [29] S. Gerstenkorn et al., *Atlas du pectre d'absorption de la molecule d'iode* (CNRS, Paris, 1978); S. Gerstenkorn et al., *Rev. Phys. Appl.* 14, 791(1979).
- [30] G. Baumgartner, H. Kornmeier, and W. Preuss, *Chem. Phys. Lett.* 107, 13(1984).
- [31] A. Hansson (private communication).
- [32] J. Sagle, R. K. Namioka, and J. Huennekens, *J. Phys. B* 29, 2629(1996).